

A Checkpoint Protein That Scans the Chromosome for Damage at the Start of Sporulation in *Bacillus subtilis*

Michal Bejerano-Sagie,^{1,2} Yaara Oppenheimer-Shaanan,^{1,2} Idit Berlatzky,¹ Alex Rouvinski,¹ Mor Meyerovich,¹ and Sigal Ben-Yehuda^{1,*}

¹Department of Molecular Biology, Faculty of Medicine, POB 12272, The Hebrew University of Jerusalem, 91120, Jerusalem, Israel
²These authors contributed equally to this work.

*Contact: sigalbe@md.huji.ac.il

DOI 10.1016/j.cell.2006.03.039

SUMMARY

In response to DNA damage, cells activate checkpoint signaling cascades to control cell-cycle progression and elicit DNA repair in order to maintain genomic integrity. The sensing and repair of lesions is critical for *Bacillus subtilis* cells entering the developmental process of sporulation as damaged DNA may prevent the cells from completing spore morphogenesis. We report the identification of the protein DisA (DNA integrity scanning protein, annotated Yack), which is required to delay the initiation of sporulation in response to chromosomal damage. DisA is a nonspecific DNA binding protein that forms a single focus, which moves rapidly within the bacterial cell, pausing at sites of DNA damage. We propose that the DisA focus scans along the chromosomes searching for lesions. Upon encountering a lesion, DisA delays entry into sporulation until the damage is repaired.

INTRODUCTION

The Gram-positive soil bacterium *Bacillus subtilis* can undergo a complex developmental process that culminates in the formation of a dormant cell type called the spore. Upon entry into sporulation, *B. subtilis* replicates its chromosome and remodels the daughter chromosomes into an elongated axial filament structure. Subsequently, an asymmetrically positioned (polar) septum is formed that divides the developing cell (sporangium) into progeny of unequal size, referred to as the forespore (the small compartment) and the mother cell. The forespore ultimately becomes the spore, whereas the mother cell nurtures the developing spore until it is discarded by lysis once morphogenesis is complete (Piggot and Losick, 2001; Errington, 2003; Piggot and Hilbert, 2004). This morphological

process is a powerful system for studying mechanisms that control cell division and development.

The differentiation of vegetative cells into spores is initiated by integrating a wide range of environmental and physiological signals. These signals are channeled into a multicomponent phosphorelay that is responsible for the phosphorylation of a key transcriptional regulatory protein, Spo0A. Spo0A, a member of the response regulator family of two-component regulatory systems, obtains its phosphate from at least three histidine protein kinases that transfer phosphate to the relay protein Spo0F, then to Spo0B, and finally to Spo0A. This regulatory hierarchy provides multiple targets for controlling a gradual initiation of sporulation (Sonenshein, 2000; Perego and Hoch, 2001; Piggot and Hilbert 2004). The phosphorylated form of Spo0A directly controls the expression of more than 120 genes (Molle et al., 2003), including genes that are involved in remodeling the sister chromosomes into an axial filament structure (Pogliano et al., 2002; Ben-Yehuda et al., 2003), genes that are required for the formation of the polar septum (Levin and Losick, 1996; Ben-Yehuda and Losick, 2002), and genes that encode key developmental regulators (Piggot and Losick, 2001; Errington, 2003; Piggot and Hilbert, 2004).

One of the important physiological requirements for entry into sporulation is the presence of an intact replicated chromosome. Conditions or mutations that result in disruption of DNA replication, defects in chromosome partitioning, or damaged DNA can delay sporulation at the level of Spo0A activation (Ireton and Grossman, 1992; Ireton et al., 1993; Lemon et al., 2000; Burkholder et al., 2001; Shafikhani et al., 2004). The best-studied example is the coupling between the initiation of sporulation and DNA replication that was found to be mediated by the *sda* gene. *sda* is activated upon a block in DNA replication and encodes a small protein that binds to and inhibits the activity of KinA, a histidine kinase that lies at the top of the phosphorelay involved in the activation of Spo0A. Thus, Sda is part of a checkpoint that ensures faithful replication of the chromosomes before entry into the developmental program of sporulation (Burkholder et al., 2001; Rowland et al., 2004).

Evidence exists for an analogous checkpoint to monitor and maintain genomic integrity. In the presence of DNA damaging agents, *B. subtilis* fails to initiate sporulation (Iretton and Grossman, 1994); thus sporulating cells must somehow sense and repair DNA damage in order to accomplish faithful generation of the two cell types. However, the mechanism underlying this DNA-damage checkpoint is not well understood. Here we describe the identification of DisA (for DNA integrity scanning protein, annotated YacK), which is involved in monitoring genomic integrity at the onset of sporulation. In the absence of DisA, cells enter sporulation even in the presence of chromosomal lesions, resulting in fewer viable spores compared with wild-type cells. We provide evidence that DisA molecules are organized into focal assemblies that move dynamically within bacterial cells, scanning the DNA for the presence of lesions. When damage is encountered, DisA pauses at the lesion site and induces a cellular response that culminates in a temporary block in sporulation. We propose that DisA prevents cells from entering spore morphogenesis under conditions in which they cannot successfully form mature spores and, hence, may perish trying.

RESULTS

DisA Participates in a DNA-Damage Checkpoint That Is Active at the Onset of Sporulation

DisA was discovered in a search for proteins that interact with RacA, which is produced at the onset of sporulation and is involved in axial filament formation and asymmetric division (Ben-Yehuda et al., 2003) (see Experimental Procedures). However, we observed that axial filament formation and polar division were unperturbed in a strain (YA5) harboring a *disA* null mutation, indicating that *disA* is not involved in executing these processes. These observations prompted us to consider other roles for DisA. *disA* is the last gene in an operon that contains six genes involved in protein degradation, competence, and DNA repair (Kruger et al., 1996). We found that deletion of the *disA* gene has no detectable effect on cell division, sporulation, competence, or response of vegetative cells to DNA damage (data not shown). Next, we examined whether DisA is involved in responding to DNA damage during sporulation. Wild-type and DisA mutant cells were treated with different concentrations of nalidixic acid (nalidixic acid targets DNA gyrase and therefore causes DNA damage) at the onset of sporulation, and spore formation was assayed by heat resistance. In untreated cultures, the resulting number of heat-resistant, colony-forming units (spores) was similar to that of the wild-type. In contrast, in the presence of nalidixic acid, the number of spores produced by the mutant was significantly lower than that of the wild-type (Figure 1A). Similar results were observed when the cells were exposed to the DNA-damaging agent Mitomycin C (MMC) (Figure S1A).

To visualize the developmental progression of the nalidixic acid-treated cells, we monitored sporulation by fluorescence microscopy. In comparison to untreated cells,

treated cells of both the wild-type and the DisA mutant were delayed in their entry into sporulation, as judged by reduced numbers of asymmetric septa 2.5 hr after treatment (Figures 1B and 1C). However, by 3.5 hr after treatment, a significant percentage (15%) of the mutant cells had entered sporulation, whereas less than 2% of the wild-type cells had undergone asymmetric division (Figures 1B and 1C). This phenotype was observed over a range of concentrations of nalidixic acid or when the cells were exposed to MMC (Figures 1C and S1, respectively). Thus, although DisA mutant cells are less efficient in producing mature spores, they are able to enter sporulation earlier than wild-type cells in the presence of DNA damage.

We also examined the expression of early sporulation genes (*spoIIIE* and *racA*), which are synthesized prior to asymmetric division under the control of the transcription factor Spo0A (York et al., 1992; Ben-Yehuda et al., 2003). Wild-type and DisA mutant cells harboring *spoIIIE-lacZ* or *PracA-lacZ* reporter fusions were induced to sporulate in the presence or absence of nalidixic acid, and β -galactosidase activity was monitored (Figures 2A–2D). In the absence of nalidixic acid, Spo0A activity was indistinguishable between the wild-type and the mutant cells (Figures 2A and 2B). The addition of nalidixic acid greatly reduced Spo0A activity in both the wild-type and the mutant cells. Importantly, in agreement with our cytological analysis, in DisA mutant cells β -galactosidase activity was observed earlier and reached higher levels in comparison to the wild-type cells (Figures 2C and 2D). Similar results were obtained when the production of SpoIIIE-GFP and RacA-GFP fusions was examined by fluorescence microscopy (Figure S2 and data not shown). Thus, we concluded that DisA is required, at least in part, to inhibit Spo0A activity when DNA is damaged.

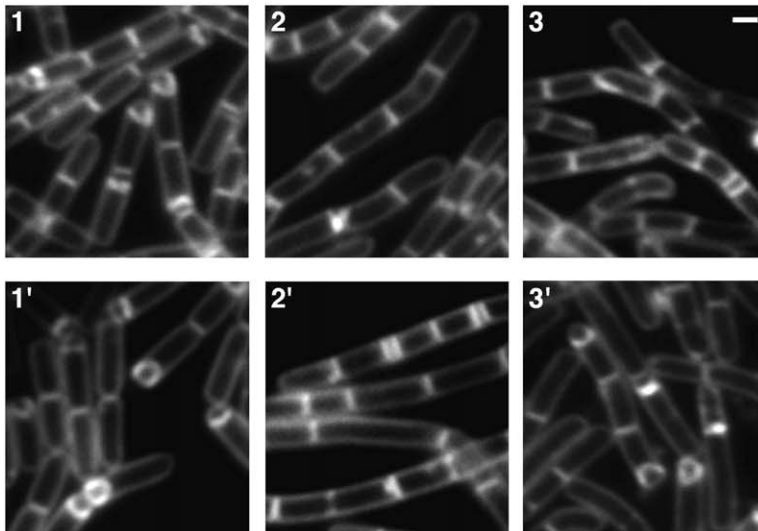
The Spo0A transcription factor is activated by phosphorylation and obtains its phosphate by a phosphorelay consisting of histidine kinases (KinA, B, and C) and the phosphotransfer proteins Spo0F and Spo0B (see Introduction). To investigate whether DisA acts by modulating the phosphorylation state of Spo0A, we introduced an allele of *spo0A* (*rvtA11*) that bypasses the requirement for the normal phosphorylation pathway (Sharrock et al., 1984; LeDeaux and Grossman, 1995) into wild-type and DisA mutant backgrounds. Spo0A activity was monitored by the use of *spoIIIE-lacZ* or *PracA-lacZ* reporters in the presence or absence of nalidixic acid. As shown in Figure 2, cells harboring the altered form of Spo0A were much less sensitive to the presence of nalidixic acid and produced β -galactosidase at levels that were almost comparable to those seen in untreated cells (Figures 2E and 2F). Moreover, under these conditions, no significant difference was observed between the wild-type and the DisA mutant cells. These results indicate that DisA delays sporulation by affecting the phosphorylation state of Spo0A.

Taken together, our findings are consistent with the idea that DisA participates in a DNA-damage checkpoint that is active prior to asymmetric division and delays Spo0A

A

Strain	Genotype	Nalidixic acid ($\mu\text{g/ml}$)	Spores (%)
PY79	wild-type	0	94.90
YA5	$\Delta\text{disA}::\text{tet}$	0	87.50
MB3	<i>disA-gfp-spc</i>	0	89.20
PY79	wild-type	350	13.40
YA5	$\Delta\text{disA}::\text{tet}$	350	0.90
MB3	<i>disA-gfp-spc</i>	350	12.50
PY79	wild-type	500	0.05
YA5	$\Delta\text{disA}::\text{tet}$	500	0.01
MB21	<i>amyE::P_{hyper-spank}-disA-spc</i> (-IPTG)	0	85.60
MB21	<i>amyE::P_{hyper-spank}-disA-spc</i> (+IPTG)	0	12.50

B



C

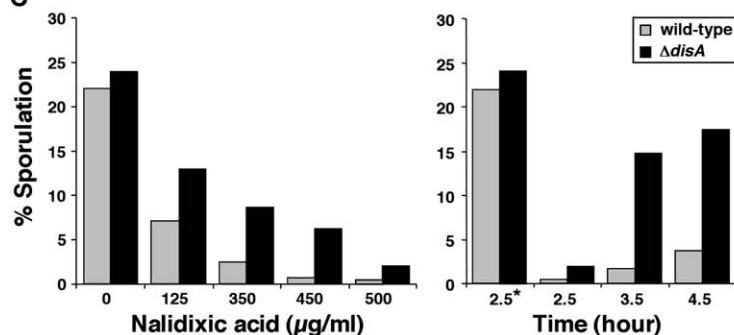


Figure 1. DisA Induces a DNA-Damage Checkpoint Response

(A) Strains were induced to sporulate in DS sporulation medium for 24 hr. The percentage of sporulation was determined as the ratio of heat resistant colony-forming units to the total colony-forming units. The percentage of sporulation in the presence of nalidixic acid was normalized to that of untreated cultures. Nalidixic acid was added at hr 0 of sporulation at the indicated concentrations. IPTG (Isopropyl- β -D-thiogalactopyranoside) was added at hr 0 of sporulation at a final concentration of 0.5 mM. (B) Fluorescence microscopy images of cells from strains PY79 (wild-type) (images 1–3) and YA5 ($\Delta\text{disA}::\text{tet}$) (images 1'–3'); without nalidixic acid at hr 2.5 of sporulation (images 1 and 1'); and with 500 $\mu\text{g/ml}$ nalidixic acid at hr 2.5 (images 2 and 2') and at hr 4.5 (images 3 and 3') of sporulation. The cells were treated with the membrane stain FM1-43. Scale bar corresponds to 1 μm .

(C) Quantitation analysis of representative experiments with PY79 (wild-type) and YA5 ($\Delta\text{disA}::\text{tet}$) sporulating cells as visualized by fluorescence microscopy. Left: Various concentrations of nalidixic acid were added at hr 0 of sporulation, and the cells were visualized at hr 2.5. Right: time-course analysis of cells undergoing sporulation in the absence (*) or presence of 500 $\mu\text{g/ml}$ nalidixic acid. At least 600 cells were counted for each time point.

activation. The absence of this checkpoint in the presence of DNA damage leads to premature entry into sporulation and consequently to impaired sporulation. In keeping with

this model, overproduction of DisA was found to reduce polar division and to decrease sporulation efficiency (Figure 1A and data not shown).

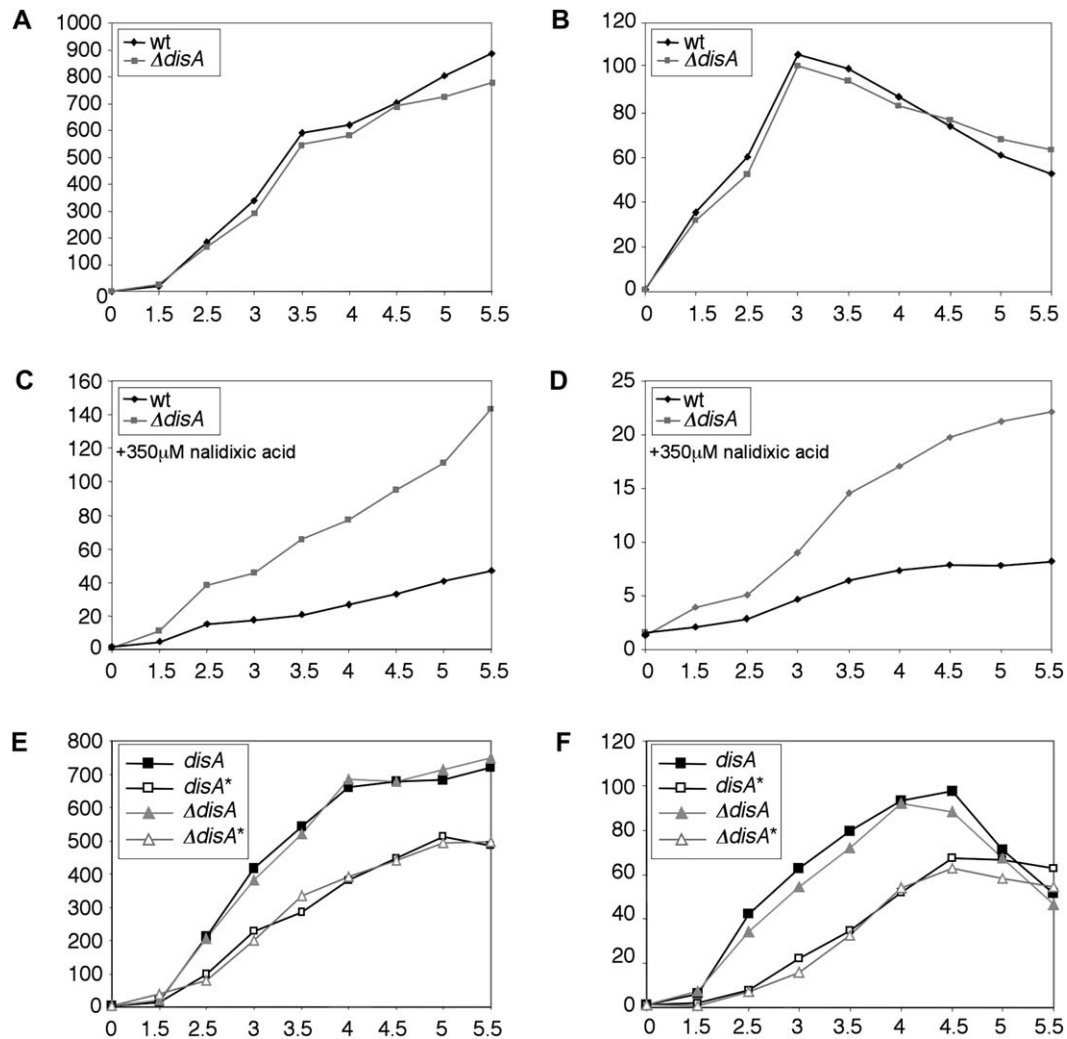


Figure 2. DisA Affects Spo0A Activation in the Presence of DNA Damage

(A–D) β -galactosidase activity assay from wild-type (black) and $\Delta disA::tet$ (gray) strains harboring the *spoIIE-lacZ-cat* (A and C) or the *amyE::P_{racA}-lacZ-cat* (B and D) reporters. Note the different scales of β -galactosidase activity in the four panels.

(A and B) Untreated cells.

(C and D) Nalidixic acid-treated cells. Nalidixic acid (350 μ g/ml) was added at hr 0 of sporulation.

(E and F) β -galactosidase activity assay from strains harboring the *vrtA11* allele with (black) or without (gray) the *disA* gene in the presence (*) or absence of nalidixic acid (350 μ g/ml). Nalidixic acid was added at hr 0 of sporulation.

(E) Strains bearing the *spoIIE-lacZ-cat* reporter.

(F) Strains bearing the *amyE::P_{racA}-lacZ-cat* reporter.

Samples were taken at the indicated time points (hours) after suspension in sporulation medium, and β -galactosidase activity was calculated in Miller units.

DisA Forms a Highly Dynamic Focus at the Onset of Sporulation

To investigate the subcellular localization of the checkpoint protein, we constructed a strain (MB3) harboring a *disA-gfp* gene fusion in place of the wild-type gene. Growth and sporulation of MB3 were indistinguishable from that of the wild-type. Importantly, the DisA-GFP protein was fully functional because sporulating MB3 cells were as sensitive to nalidixic acid as were wild-type cells (Figure 1A). DisA-GFP was seen as a single discrete glob-

ular focus that colocalized with the bulk of the DNA in cells that were induced to sporulate. This localization pattern was apparent both before and after the formation of the polar septum (Figure 3A). To examine whether these DisA-GFP foci reflect the proper localization of the endogenous protein, we carried out immunofluorescence microscopy using antibodies to DisA on cells producing unmodified wild-type DisA. The immunostaining pattern closely resembled that observed with DisA-GFP (Figure 3B). We observed little or no immunostaining in the

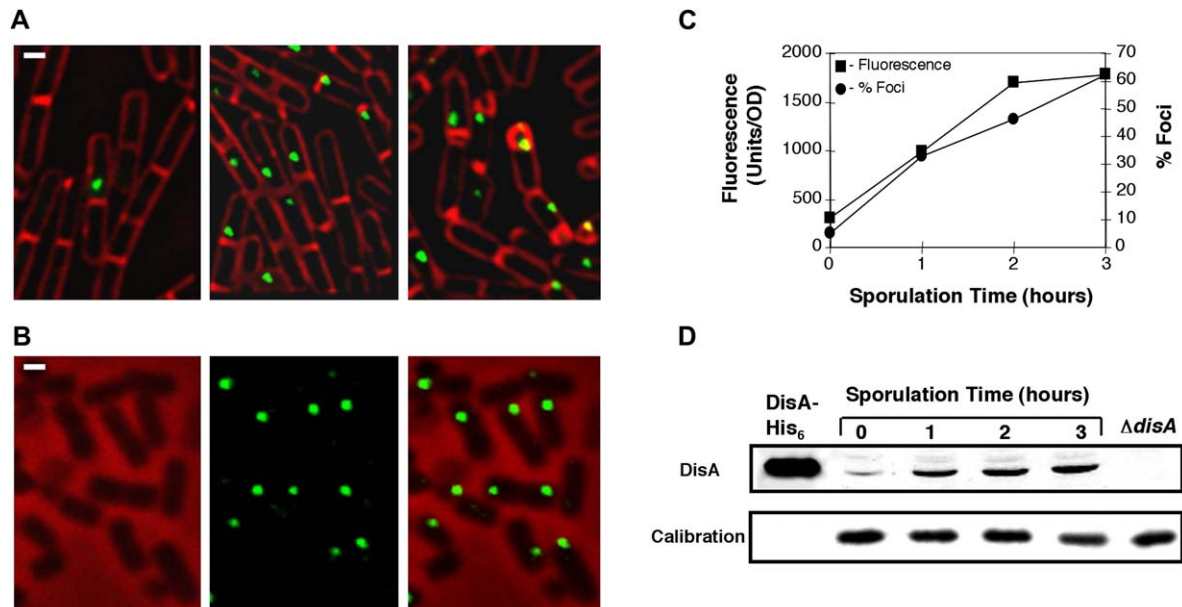


Figure 3. DisA Forms Foci upon Entry to Sporulation

(A) Shows FM4-64-stained cells (red) from a DisA-GFP-producing strain (MB3). DisA-GFP (green) is seen as foci. Shown are MB3 cells at hr 0 (left image), hr 1 (middle image), and hr 2 (right image) of sporulation.

(B) Phase contrast (red, left), immunofluorescence staining (green, middle), and overlay (right) images of sporangia from a wild-type strain (PY79) that had been collected and fixed at hr 1.5 of sporulation. The cells were treated with anti-DisA antibodies. Scale bars correspond to 1 μ m.

(C) Shows the % of MB3 cells displaying DisA-GFP fluorescence foci during sporulation as well as the corresponding total fluorescence values (arbitrary units).

(D) Immunoblot analysis with polyclonal anti-DisA antibodies that was carried out with extracts from wild-type cells (PY79) collected at hr 0, 1, 2, and 3 of sporulation. An extract prepared from a DisA mutant strain (YA5) at hr 2 of sporulation was used as a control. 0.5 μ g of purified DisA-His₆ was loaded as a size marker. A nonspecific band was used as a loading control (lower panel).

DisA mutant control (data not shown). Thus, DisA localizes as a discrete focus at the onset of sporulation.

The number of cells exhibiting a DisA-GFP focus increased dramatically after suspension in sporulation medium (Figures 3A and 3C). More specifically, 5% of the cells displayed a DisA-GFP focus at time 0. As early as 1 hr after suspension, 33% of the cells exhibited a focus, and 46% had a focus at hr 2. The increase in the number of cells harboring a DisA-GFP focus correlated with a total increase in fluorescence intensity as well as with an elevation in wild-type DisA protein levels (Figures 3C and 3D, respectively) and therefore reflected induced production of DisA. This observation prompted us to investigate whether DisA synthesis is dependent on Spo0A, the master transcriptional regulator for entry into sporulation. Our experiments indicate that induction of *disA* expression upon initiation of sporulation was not dependent on this regulator (data not shown). Similar results were obtained in the absence of sigma H, an additional transcription factor that is required to initiate sporulation (Piggot and Losick, 2001). In addition, we observed an increase in the number of cells expressing DisA-GFP at a high cell density in a rich medium (data not shown). Thus, it seems likely that *disA* is induced by non-sporulation-specific regulatory proteins at the end of the exponential growth phase and, as shown above, acts upstream of Spo0A and modulates its activity. Inter-

estingly, another gene in the *disA* operon, *clpC*, encodes a protease subunit that degrades an antsporulation transcription factor early in development (Pan et al., 2001), suggesting that the entire operon is involved in early sporulation events.

To study the movement of DisA-GFP foci, we analyzed the fusion protein by time-lapse microscopy. Sporulating MB3 cells were applied to an agarose pad on a glass slide and photographed at 200–400 msec intervals. We observed that the foci are remarkably dynamic, rapidly traversing the entire cell in a few seconds (Figures 4A and 4B; Movies S1, S2, and S5). Single-particle tracking analysis revealed that the average focus speed was 0.22 μ m/sec at room temperature (Figure S3). Importantly, this unusual movement was abolished when the cells were fixed with formaldehyde (Movie S6). Moreover, when the cells were treated with the ATPase inhibitor sodium azide, the DisA-GFP foci were immediately stalled, implying that DisA mobility is energy dependent (Movies S7A and S7B).

A closer investigation of the time-lapse microscopy movies revealed that when two daughter cells were separated by a yet incomplete septum (as indicated by the membrane staining), the focus was able to cross from one compartment to the other, both during medial and polar divisions (Figures 4C and 4D; Movies S3 and S4). This observation led us to infer that when the septum is

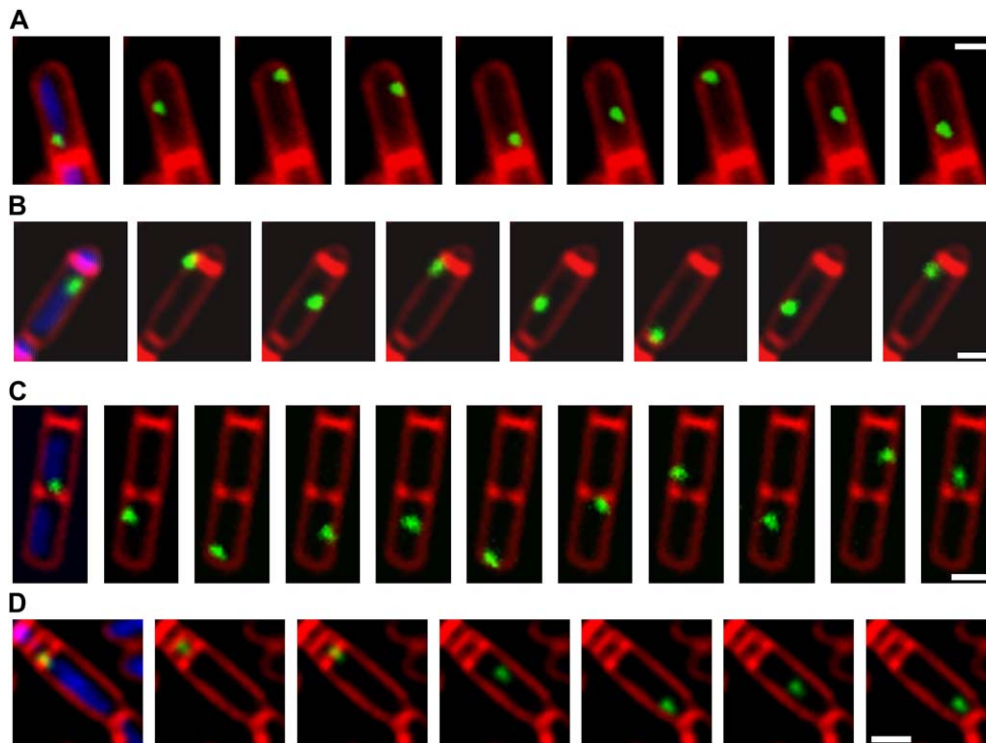


Figure 4. DisA Forms Highly Dynamic Foci

(A–D) The dynamic localization of DisA-GFP foci is demonstrated by time-lapse microscopy from individual cells of the DisA-GFP-producing strain (MB3) before (A and C) and after (B and D) polar division. Cells were stained with FM4-64 (red) and DAPI (blue) and photographed at 200–400 msec intervals. Selected images were chosen for demonstration. The corresponding movies are displayed in the [supplemental data \(Movies S1–S4\)](#). Scale bars correspond to 1 μm .

sealed upon completion of division, the DisA-GFP focus becomes trapped in one of the two compartments. Consequently, DisA becomes distributed unequally upon division between the two daughter cells. Consistent with this notion, only one particle is usually observed per sporangium after polar division, and it is chiefly found in the larger mother cell compartment.

DisA Focus Movement Depends on Chromosome Integrity

We reasoned that if the role of DisA is to monitor for DNA damage, DisA movement might be affected by DNA lesions. To test this possibility, we visualized DisA-GFP movement in the presence of nalidixic acid. Indeed, we found that the majority of the DisA-GFP foci were no longer moving and were stationary at various positions within the cells ([Movie S8](#)). Similar results were obtained when the cells were treated with MMC (see below). These data suggest that the movement of the DisA focus ceases in the presence of DNA lesions. These DNA-damaging agents produce multiple lesions that may result indirectly in stalled DisA-GFP foci. To obtain stronger evidence for a direct connection between chromosomal integrity and DisA-GFP foci movement, we constructed a DisA-GFP-producing strain in which we could induce a site-specific

double strand break. This was achieved by generating DisA-GFP strains that produced the yeast homothallic switching endonuclease (HO) ([Haber, 1998](#)) under an inducible promoter, with and without the HO recognition sequence (YA41 and YA57, respectively). The recognition sequence was inserted close to the origin of replication that is located in the vicinity of the cell pole at the onset of sporulation ([Webb et al., 1997](#)). The inducer was added upon suspension in sporulation medium, and the localization pattern of DisA-GFP was examined 1.5 hr after induction. In the absence of the recognition site (YA57), DisA-GFP foci were highly mobile and moved in a similar manner to the foci in untreated cells (data not shown). In contrast, in the presence of the HO recognition site (YA41), the movement of DisA-GFP was abolished in the majority of cells (86%) upon induction of the endonuclease ([Figure 5A](#); [Movie S9](#)). However, unlike the random positions of stalled DisA-GFP foci observed in MB3 cells treated with DNA-damaging agents, in YA41 cells the stalled DisA-GFP foci appeared to be localized at a particular site on the chromosome close to the cell pole, presumably at the HO-induced break site. In support of this idea, when the HO cut-site was inserted at a distinct chromosomal location near the terminus region, the foci position was altered and they were stalled mostly at the mid-cell position in between the two

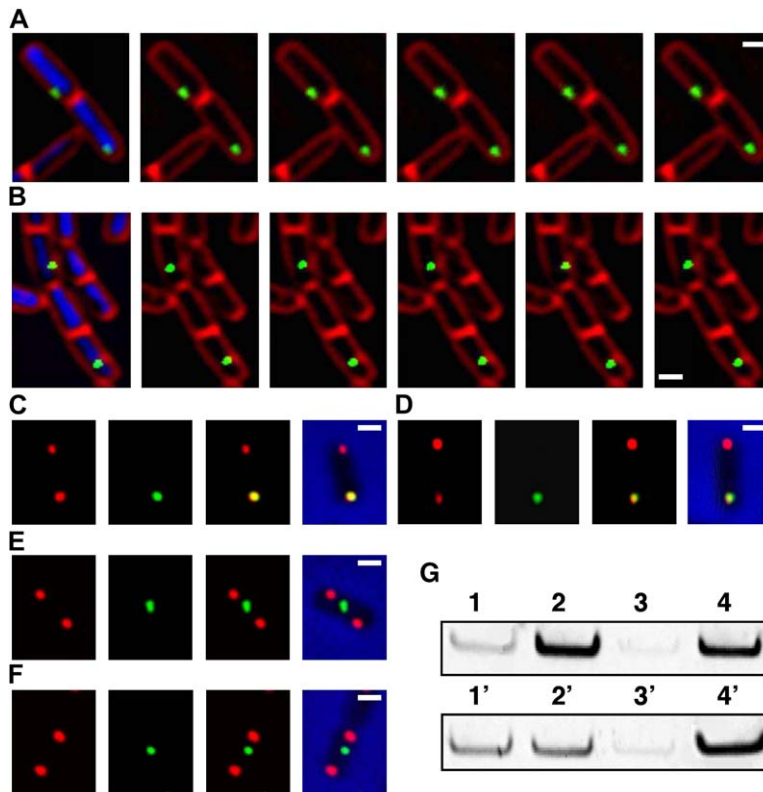


Figure 5. DisA Focus Pauses at Sites of DNA Lesion

(A and B) Time-lapse microscopy images (200–400 msec intervals) from DisA-GFP-producing strains stained with FM4-64 (red) and DAPI (blue). DisA-GFP (green) is seen as foci. Scale bars correspond to 1 μ m.

(A) YA41 (*disA-gfp-spc*, *amyE::HO_{cut-site}-cat*, *thrC::P_{spac}HO_{endo}-erm*) cells at hr 1.5 of sporulation after induction of the HO endonuclease (0.5 mM IPTG was added at hr 0). See corresponding movie (Movie S9).

(B) YA60 (*disA-gfp-kan*, *ctpA::HO_{cut-site}-spc*, *thrC::P_{spac}HO_{endo}-erm*) cells at hr 1.5 of sporulation after the induction of the HO endonuclease (0.5 mM IPTG was added at hr 0).

(C–F) YA41 (*disA-gfp-spc*, *amyE::HO_{cut-site}-cat*, *thrC::P_{spac}HO_{endo}-erm*) (C and D) and YA38 cells (*disA-gfp-spc*, *amyE::HO_{cut-site}-cat*) (E and F) were induced to sporulate in the presence of 0.5 mM IPTG. At hr 1.5 of sporulation, the cells were fixed and subjected to FISH analysis (see Experimental Procedures). Red fluorescence foci represent the *amyE* region adjacent to the DNA break site. The cells were then subjected to immunofluorescence staining using an anti-GFP monoclonal antibody to visualize the subcellular localization of the DisA foci (green). Also shown are overlays of signals from FISH and immunofluorescence with or without phase contrast images (blue). Scale bars correspond to 1 μ m. At least 400 foci were scored for each strain in two independent experiments.

(G) Cells from strains YA36 (*amyE::HO_{cut-site}-cat*) (lanes 1 and 1'), YA51 (*amyE::HO_{cut-site}-cat*, *thrC::P_{spac}HO_{endo}-erm*) (lanes 2 and 2'), and YA52 (Δ *disA::tet*, *amyE::HO_{cut-site}-cat*, *thrC::P_{spac}HO_{endo}-erm*) (lanes 3 and 3') were induced to sporulate in the presence of 0.5 mM IPTG. At hr 1.5, cells were fixed with 3.7% formaldehyde and subjected to CHIP analysis (see Experimental Procedures). The DNA recovered from the CHIP was used as a template for quantitative PCR reactions. The PCR products were resolved on a 12% polyacrylamide gel. The gel was stained using SYBRgreen I Nucleic acid gel stain (Molecular Probes) and visualized with Image Master VDS-CL (Amersham). MetaMorph software was used to quantitate band intensities. Shown are PCR fragments amplified from two different chromosomal loci: *amyE* locus (lanes 1–4), which is adjacent to the HO-induced DNA break site, and the unrelated *racA* locus (lanes 1'–4'). Total chromosomal DNA (the DNA before immunoprecipitation) from YA51 was used as a positive control for the PCR reactions (lanes 4 and 4'). To account for differences in loading or the variations in amplification with different primer sets, enrichment factor was normalized as: (band intensity of the *amyE* IP) / (band intensity of the *racA* IP). The enrichment factors for YA36 and YA51 were 0.47 and 7.46, respectively.

chromosomal copies where the terminus is generally located (Webb et al., 1997) (Figure 5B).

To independently examine whether the DisA focus is recruited to the site of DNA damage, we carried out fluorescence in situ hybridization (FISH) to visualize the DNA break site concomitantly with immunofluorescence microscopy to localize the DisA focus (see Experimental Procedures). Sporulating cells producing the HO endonuclease (YA41) were fixed and hybridized with a fluorescent probe corresponding to a 15kb region adjacent to the HO cut-site. The chromosomal region appeared as a distinct fluorescent focus with one or two foci per cell (examples are shown in Figures 5C–5F). These cells were then subjected to immunofluorescence microscopy to localize the DisA focus. In 66.7% of the cells bearing a DisA focus, the focus clearly colocalized with the DNA break site (examples are shown in Figures 5C and 5D). By comparison, only 12.1% of the DisA foci colocalized with the HO

cleavage site in a control strain that did not produce the HO endonuclease (examples are shown in Figures 5E and 5F).

In a complementary approach, we used Chromatin Immunoprecipitation (ChIP) to determine whether DisA resides in close proximity to the DNA break site. Extracts were prepared from sporulating cells (either producing or not producing the HO endonuclease) that had been treated with formaldehyde, which cross links proteins to DNA. DisA-DNA complexes were then immunoprecipitated using anti-DisA antibodies, and the DNA from the immunoprecipitation was recovered and used as a template for quantitative PCR reactions. Consistent with the idea that DisA scans along the chromosome, in the absence of the HO endonuclease (and therefore in the absence of DNA lesions) (YA36), we obtained efficient precipitation of all chromosomal locations examined (Figure 5G and data not shown). As a control, very little signal was

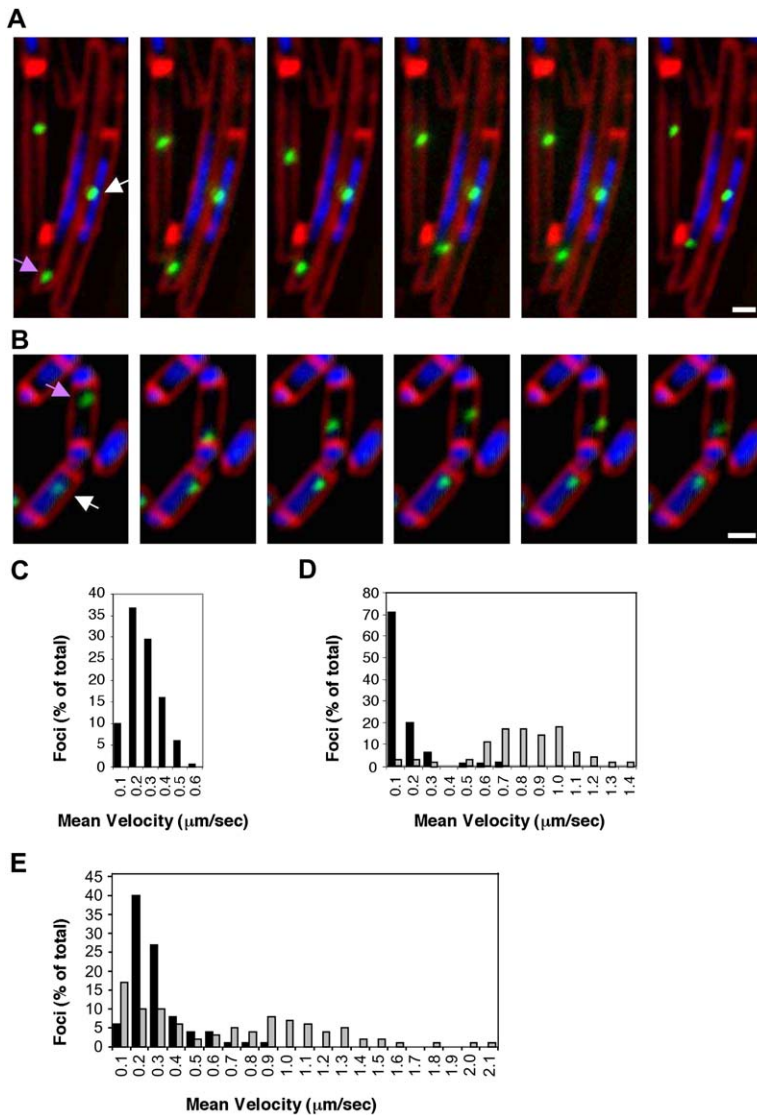


Figure 6. DNA Is Not Required for DisA Focus Movement

(A and B) Time-lapse microscopy images (200–400 msec intervals) from DisA-GFP-producing strains stained with FM4-64 (red) and DAPI (blue). DisA-GFP (green) is seen as foci. White arrows point to DisA-GFP foci colocalized with DNA, and purple arrows indicate DisA-GFP foci in DNA-free cellular regions. Scale bars correspond to 1 μ m.

(A) MB3 (*disA-gfp-spc*) cells treated with MMC (25 ng/ml) and visualized at hr 1.5 of sporulation. See corresponding movie (Movie S10).

(B) MB15 (*disA-gfp-spc, spoIIAC::kan*) cells at hr 3 of sporulation. See corresponding movie (Movie S11).

(C–E) Single-particle tracking analyses of DisA-GFP foci in individual cells (MetaMorph, Universal Imaging).

(C) Untreated MB3 cells at hr 1.5 of sporulation. (D) MB3 cells treated with MMC (as in A) at hr 1.5 of sporulation.

(E) MB15 cells at hr 3 of sporulation. At least 200 foci were examined for each analysis. Foci that colocalized with the DNA and foci in DNA-free regions are shown in black and gray bars, correspondingly.

detected when the ChIP procedure was carried out with sporulating cells from a DisA mutant (YA52) (Figure 5G and data not shown). When the ChIP procedure was performed with cells producing the HO endonuclease (YA51), preferential binding by DisA was clearly observed at the lesion site (an enrichment factor of 7.46 in YA51 in comparison with an enrichment factor of 0.47 in YA36; Figure 5G), consistent with our cytological experiments.

In summary, the evidence indicates that DisA interacts with DNA and rapidly scans along the chromosomes during sporulation and that its rapid motion is abrogated by the presence of DNA lesions. In support of our proposal, sequence analysis of DisA predicts a putative Helix-hairpin-Helix (HHH) DNA binding domain at its C terminus (Doherty et al., 1996). Moreover, gel retardation experiments using purified recombinant DisA showed that DisA binds DNA with a moderate affinity (approximate K_d : 10^{-8} M) and with no apparent sequence specificity (Figure S4).

DNA Is Not Required for DisA Focus Movement

Our data suggest that DisA tracks along the DNA. To determine whether DisA-GFP movement requires DNA, cells were needed that lack DNA but still harbor DisA-GFP foci. Such cells are formed in response to MMC treatment, which perturbs DNA segregation and leads to a high frequency of anucleate cells and elongated cells, where the DNA occupies only a portion of the cell. We examined DisA-GFP foci in sporulating cells treated with MMC and found that the foci were readily detected both on the DNA and in DNA-free parts of the cells (Figure 6A). Although DisA-GFP foci that colocalized with DNA were stalled, DisA-GFP foci located in parts lacking DNA were capable of moving rapidly (Figures 6A, 6C, and 6D; Movie S10). Another system that allows us to examine DNA-free cells is mutant sporangia that form bipolar septa due to a mutation in the sporulation gene *spoIIAC* (Piggot and Losick, 2001). In such a “disporic” mutant, each forespore

compartment receives a chromosome, whereas the mother cell remains anucleate. We observed that the DNA-free mother cell frequently contained DisA-GFP foci in sporulating *spolIAC* mutant cells. Moreover, the majority of these foci were highly dynamic within the empty compartment (Figure 6B; Movie S11). Single-particle tracking analysis indicates that foci movement within the DNA-free compartment is in general more rapid than foci movement in the presence of DNA (Figure 6E). Importantly, the rapid movement of the foci observed in the absence of the DNA in these two DNA-free systems was energy dependent as it was abolished by treating the cells with sodium azide (Figure S5 and data not shown). The simplest interpretation of our experiments is that DNA is not required for DisA focus movement, but the presence of DNA (and even more so damaged DNA) attenuates focus motion, probably due to DisA DNA scanning activity.

The Cytoskeletal Proteins MreB and Mbl Are Not Required for DisA Focus Motion

Since DNA influences but is not necessary for DisA movement, it is likely that there are other cellular structures that facilitate DisA motion. A good candidate is the cytoskeleton, so we examined DisA-GFP movement in the absence of the two known cytoskeletal proteins, namely MreB and Mbl. Both proteins are required for maintaining cell shape in *B. subtilis* and were shown to form filamentous helical structures that lie close to the cell surface (Jones et al., 2001). Deletion of *mbl* did not have any measurable effect on the movement of DisA foci (Movie S12). In the case of MreB, since it is essential for *B. subtilis* we could only deplete the *mreB* gene product (Jones et al., 2001). Under the depleted conditions, a significant fraction of cells lost their rod shape but nevertheless maintained DisA-GFP focus movement (Movie S13). Thus, these experiments indicate that these cytoskeletal proteins do not influence significantly DisA focus motion.

DISCUSSION

We propose the following model for the DNA-damage checkpoint response that is mediated by DisA. Upon sensing sporulation conditions, DisA expression level increases. After reaching a critical cellular concentration, DisA molecules gather to form a globular structure that moves rapidly over the chromosome searching for lesions. The rapid movement of this large complex enables DisA to quickly scan many chromosomal sequences. The nonspecific DNA binding activity of DisA is responsible for its ability to scan through the chromosome rapidly. Once a lesion is present on the DNA, either the lesion itself or the associated repair proteins act as a physical blockage that perturbs DisA complex mobility and causes its arrest at the lesion site. This stalled DisA triggers a cellular response that culminates in a temporary block to initiating sporulation. The arrest is relieved when the DNA is repaired or by other as yet to be identified signals.

Surveillance systems that respond to chromosomal damage by shutting down cell-cycle and developmental processes have been well characterized in eukaryotic cells (Weinert and Hartwell, 1988; Li and Zou, 2005; Lisby and Rothstein, 2005), but little is known about analogous checkpoint mechanisms in prokaryotes. Here we show that in DisA mutant cells the expression of early sporulation genes and the formation of the polar septum are partially uncoupled to the DNA-damage response, implying that DisA helps to stall sporulation when DNA is damaged. DisA is expressed at an early stage of sporulation, affects the expression of Spo0A regulated genes, and presumably acts through regulating the Spo0A phosphorylation state as occurs in the Sda pathway (Burkholder et al., 2001). It is possible that DisA acts upstream of Sda, but our preliminary experiments suggest that *disA* and *sda* act in parallel genetic pathways (data not shown). Moreover, previous evidence supports the view that sporulating cells sense DNA replication and DNA damage by different mechanisms (Iretton and Grossman, 1994). It is also clear from our data that sporulating cells still respond to DNA damage, even in the absence of DisA, suggesting that there may be parallel DNA-damage checkpoint pathways that operate in a DisA independent manner and are activated at the onset of sporulation.

Many questions concerning the mechanism of DisA motion and the proposed signaling remain unanswered and will be the subject of further study. We do not understand how the DisA complex traces DNA or how its path is determined. It is tempting to speculate that DisA moves on tracks that are analogous to the eukaryotic cytoskeleton. The energy source that we demonstrated to be required for DisA movement remains to be identified. It seems likely that a nucleotide binding protein interacts with DisA to provide the driving force for the scanning complex. It is notable that the neighboring gene in the *disA* operon encodes a protein that contains an ATP binding domain (*radA*). However, in preliminary studies where DisA-GFP was synthesized from an ectopic chromosomal site, we found that deletion of *radA* had no significant effect on DisA mobility. It also remains elusive whether DisA is part of a large “scansome” complex or if it is the sole constituent of the DNA-scanning foci. It is possible that many different complexes that scan the DNA for lesions exist and that each has a separate role.

The discovery that DisA focus pauses at sites of the DNA damage raises the question as to whether DisA recognizes the lesion itself, an intermediate repair processing product, or the associated repair proteins. According to our data, the formation of a double strand break stalls the DisA focus movement, and we assume that this pausing induces the DisA-checkpoint. However, preliminary data in our laboratory suggest that lesions caused by UV irradiation (or by a drug that mimics UV irradiation) do not activate the DisA-checkpoint efficiently, suggesting that the nature of the lesion (or its associated proteins) may determine the type of the checkpoint cellular response.

Aggregation of repair and DNA-damage checkpoint proteins into cytological foci at the damage site have been previously described for eukaryotes and prokaryotes (Bishop, 1994; Haaf et al., 1995; Smith et al., 2001; Lisby et al., 2003; Kidane et al., 2004; Lisby et al., 2004; Kidane and Graumann, 2005). The advantage of forming foci with high protein concentration may be the formation of a microenvironment that enhances some biochemical repair processes. The existence of a DisA focus prior to damage detection, as observed here, may make its action more effective as many DisA molecules reach at once to the site of the lesion. It has been proposed that the colocalization of checkpoint and repair proteins at repair centers in eukaryotes allows for coordination of cell-cycle progression with repair status (Lisby et al., 2004). It seems likely that a similar situation exists at the onset of development in *B. subtilis*.

Homologs to DisA exist in all *Bacilli* species sequenced to date as well as in other spore-forming bacteria such as *Clostridia* and *Streptomyces*, supporting our model that DisA has an important checkpoint role in sporulation. However, DisA homologs can also be found in some Gram-positive nonsporulating bacteria. This suggests that certain DisA homologs may have a vegetative role that could be relevant to a wide range of organisms, perhaps mediated by the ubiquitous HhH DNA binding domain and coil-coiled motif of DisA. Our proposed model for the checkpoint function of DisA is reminiscent of the situation in eukaryotes where DNA-damage checkpoint proteins have been localized to repair centers (Lisby et al., 2004). Thus, it is tempting to speculate that preexisting complexes of proteins that scan DNA and search for lesions are a cellular feature that has been conserved throughout evolution.

EXPERIMENTAL PROCEDURES

Strains

B. subtilis strains were derivatives of the wild-type strain PY79 (Youngman et al., 1984) (except for MB44) and are listed in Table S1. Plasmid constructions are described in Supplemental Data.

General Methods

Growth and sporulation were carried out at 32°C. Cells were grown in hydrolyzed casein (CH) growth medium. The cultures were inoculated at an OD₆₀₀ of 0.05 from an overnight culture in the same medium. Sporulation was induced by transferring cells growing in CH medium to the resuspension medium of Sterlini and Mandelstam (Sterlini and Mandelstam, 1969; Harwood and Cutting, 1990). β -galactosidase activity assay was performed as described by Harwood and Cutting (1990). For induction of the P_{hyper-spac}-*disA* and P_{spac}-*HO* fusions, the final IPTG concentration was 0.5 mM. Immunoblot analysis was carried out as described by Sambrook et al. (1989). Protein detection was performed using Peroxidase conjugated anti-rabbit antibody (Jackson ImmunoResearch) and EZ-ECL kit (Biological Industries, Beit Haemek, Israel) according to the manufacturer's instructions. Additional general methods were carried out as described previously (Ben-Yehuda and Losick, 2002).

Identification of DisA

We previously discovered that the process of axial filament formation is mediated by the sporulation-induced protein RacA (Ben-Yehuda

et al., 2003). In an attempt to discover novel proteins that act in concert with RacA, we carried out a two-hybrid screen using RacA as bait. We identified DisA (annotated Yack) as a potential RacA-interacting protein. Similarly to RacA, DisA has a predicted DNA binding domain and a putative coil-coiled motif. However, in cells harboring a null mutation in *disA*, the formation of the axial filament was unperturbed and the localization pattern of RacA was unaffected. Although the proteins seem to interact in vitro (yeast two-hybrid, far western), additional genetic studies failed to reveal a significant connection between RacA and DisA in vivo.

Fluorescence Microscopy

Fluorescence microscopy was carried out as previously described (Ben-Yehuda and Losick, 2002). For time-lapse microscopy observations, a chamber slide (VWR Scientific) filled with sporulation medium containing 1% agarose was used. Samples (0.5 ml) of culture were removed, centrifuged briefly, and resuspended in 10 μ l of PBS \times 1 (Phosphate-Buffered Saline) supplemented with the membrane stain FM4-64 (Molecular Probes, Eugene, OR) at 1 μ g/ml and the DNA stain 4,6-Diamidino-2-phenylindole (DAPI) (Sigma) at 2 μ g/ml. Importantly, DisA movement was not affected by the presence of DAPI (Figure S3; Movies S14A and 14B). Cells were visualized and photographed using Axioplan2 microscope (Zeiss) equipped with CoolSnap HQ camera (Photometrics, Roper Scientific). System control and image processing were performed using MetaMorph 6.2r4 software (Universal Imaging).

Immunofluorescence Microscopy

Immunofluorescence microscopy was carried out as previously described (Ben-Yehuda and Losick, 2002). The blocking solution contained 10% of an extract from a *disA* null strain. Rabbit anti-DisA antibodies were used at 1:5000 dilution, and FITC secondary antibodies (Jackson ImmunoResearch) were used at 1:200 dilution.

Fluorescence In Situ Hybridization

FISH probe was generated by PCR amplification of ten different fragments (about 1.5 kb each), which correspond to a 15-kb region adjacent to the HO cut-site located at the *amyE* locus. The primers that were used for the PCR reactions are listed in Table S2. The PCR fragments were fluorescently labeled using tetramethylrhodamine-5-dUTP (Roche) according to the manufacturer's instructions. The labeled PCR fragments were mixed and used in the FISH procedure. FISH followed by immunofluorescence microscopy is described in Supplemental Data.

Chromatin Immunoprecipitation

Chromatin IP was performed as previously described (Strahl-Bolsinger et al., 1997; Ben-Yehuda et al., 2003). Polyclonal anti-DisA antibodies from rabbit (Sigma) were produced against purified DisA-His₆. 1/5 μ l of the DNA from the immunoprecipitation was used for each reaction, and 1/5,000 μ l of the "total DNA" was used for comparison reactions. Twenty-two to twenty-five amplification cycles were performed, and the PCR products were resolved on 12% polyacrylamide gels (TBE \times 0.5). The gels were stained using SYBRgreen I Nucleic acid gel stain (Molecular Probes) and visualized with Image Master VDS-CL (Amersham). The band intensities were determined using MetaMorph 6.2r4 software (Universal Imaging). The primers that were used for the PCR reactions are listed in Table S2.

Total Fluorescence Measurements

Sporulating cells carrying DisA-GFP were induced to sporulate in resuspension medium. At different time points, 200 μ l samples were placed in a 96-well culture plates (Nunc), and the fluorescence value of each sample was measured using a fluorescence reader (FLOUstar Galaxy, bmg).

DisA purification and Electrophoretic Mobility Shift Assay (EMSA) methods are described in Supplemental Experimental Procedures.

Supplemental Data

Supplemental Data include five figures, two tables, Experimental Procedures, References, and fourteen movies and can be found with this article online at <http://www.cell.com/cgi/content/full/125/4/679/DC1/>.

ACKNOWLEDGMENTS

We thank R. Losick (Harvard University, USA), in whose laboratory the preliminary experiments for this study were performed; and J. Errington (Oxford University, UK), A. Grossman and M. Berkmen (MIT, USA), and M. Kupiec (Tel-Aviv University, IL) for strains and reagents. We thank R. Losick (Harvard University, USA), D. Rudner (Harvard Medical School, USA), D. Kearns (Indiana University, USA), A. Taraboulos (Hebrew University, IL), and members of the Ben-Yehuda laboratory for valuable comments on the manuscript. This work was supported by the Human Frontier Science Program (HFSP) Career Development Award (CDA0046/2004), by the Israel Science Foundation (ISF grant 1401/04), and by the Bruno-Goldberg Endowment to S.B.-Y.

Received: September 23, 2005

Revised: January 13, 2006

Accepted: March 11, 2006

Published: May 18, 2006

REFERENCES

- Ben-Yehuda, S., and Losick, R. (2002). Asymmetric cell division in *B. subtilis* involves a spiral-like intermediate of the cytokinetic protein FtsZ. *Cell* **109**, 257–266.
- Ben-Yehuda, S., Rudner, D.Z., and Losick, R. (2003). RacA, a bacterial protein that anchors chromosomes to the cell poles. *Science* **299**, 532–536.
- Bishop, D.K. (1994). RecA homologs Dmc1 and Rad51 interact to form multiple nuclear complexes prior to meiotic chromosome synapsis. *Cell* **79**, 1081–1092.
- Burkholder, W.F., Kurtser, I., and Grossman, A.D. (2001). Replication initiation proteins regulate a developmental checkpoint in *Bacillus subtilis*. *Cell* **104**, 269–279.
- Harwood, C.R., and Cutting, S.M. (1990). *Molecular Biological Methods for Bacillus* (New York: John Wiley and Sons).
- Doherty, A.J., Serpell, L.C., and Ponting, C.P. (1996). The helix-hairpin-helix DNA-binding motif: a structural basis for non-sequence-specific recognition of DNA. *Nucleic Acids Res.* **24**, 2488–2497.
- Errington, J. (2003). Regulation of endospore formation in *Bacillus subtilis*. *Nat. Rev. Microbiol.* **1**, 117–126.
- Haaf, T., Golub, E.I., Reddy, G., Radding, C.M., and Ward, D.C. (1995). Nuclear foci of mammalian Rad51 recombination protein in somatic cells after DNA damage and its localization in synaptonemal complexes. *Proc. Natl. Acad. Sci. USA* **92**, 2298–2302.
- Haber, J.E. (1998). Mating-type gene switching in *Saccharomyces cerevisiae*. *Annu. Rev. Genet.* **32**, 561–599.
- Ireton, K., and Grossman, A.D. (1992). Coupling between gene expression and DNA synthesis early during development in *Bacillus subtilis*. *Proc. Natl. Acad. Sci. USA* **89**, 8808–8812.
- Ireton, K., and Grossman, A.D. (1994). DNA-related conditions controlling the initiation of sporulation in *Bacillus subtilis*. *Cell. Mol. Biol. Res.* **40**, 193–198.
- Ireton, K., Rudner, D.Z., Siranosian, K.J., and Grossman, A.D. (1993). Integration of multiple developmental signals in *Bacillus subtilis* through the Spo0A transcription factor. *Genes Dev.* **7**, 283–294.
- Jones, L.J., Carballido-Lopez, R., and Errington, J. (2001). Control of cell shape in bacteria: helical, actin-like filaments in *Bacillus subtilis*. *Cell* **104**, 913–922.
- Kidane, D., and Graumann, P.L. (2005). Dynamic formation of RecA filaments at DNA double strand break repair centers in live cells. *J. Cell Biol.* **170**, 357–366.
- Kidane, D., Sanchez, H., Alonso, J.C., and Graumann, P.L. (2004). Visualization of DNA double-strand break repair in live bacteria reveals dynamic recruitment of *Bacillus subtilis* RecF, RecO and RecN proteins to distinct sites on the nucleoids. *Mol. Microbiol.* **52**, 1627–1639.
- Kruger, E., Msadek, T., and Hecker, M. (1996). Alternate promoters direct stress-induced transcription of the *Bacillus subtilis* clpC operon. *Mol. Microbiol.* **20**, 713–723.
- LeDeaux, J.R., and Grossman, A.D. (1995). Isolation and characterization of *kinC*, a gene that encodes a sensor kinase homologous to the sporulation sensor kinases KinA and KinB in *Bacillus subtilis*. *J. Bacteriol.* **177**, 166–175.
- Lemon, K.P., Kurtser, I., Wu, J., and Grossman, A.D. (2000). Control of initiation of sporulation by replication initiation genes in *Bacillus subtilis*. *J. Bacteriol.* **182**, 2989–2991.
- Levin, P.A., and Losick, R. (1996). Transcription factor Spo0A switches the localization of the cell division protein FtsZ from a medial to a bipolar pattern in *Bacillus subtilis*. *Genes Dev.* **10**, 478–488.
- Li, L., and Zou, L. (2005). Sensing, signaling, and responding to DNA damage: organization of the checkpoint pathways in mammalian cells. *J. Cell. Biochem.* **94**, 298–306.
- Lisby, M., Barlow, J.H., Burgess, R.C., and Rothstein, R. (2004). Choreography of the DNA damage response: spatiotemporal relationships among checkpoint and repair proteins. *Cell* **118**, 699–713.
- Lisby, M., Mortensen, U.H., and Rothstein, R. (2003). Colocalization of multiple DNA double-strand breaks at a single Rad52 repair centre. *Nat. Cell Biol.* **5**, 572–577.
- Lisby, M., and Rothstein, R. (2005). Localization of checkpoint and repair proteins in eukaryotes. *Biochimie* **87**, 579–589.
- Molle, V., Fujita, M., Jensen, S.T., Eichenberger, P., Gonzalez-Pastor, J.E., Liu, J.S., and Losick, R. (2003). The Spo0A regulon of *Bacillus subtilis*. *Mol. Microbiol.* **50**, 1683–1701.
- Pan, Q., Garsin, D.A., and Losick, R. (2001). Self-reinforcing activation of a cell-specific transcription factor by proteolysis of an anti-sigma factor in *B. subtilis*. *Mol. Cell* **8**, 873–883.
- Perego, M., and Hoch, J. (2001). Two-component systems, phosphorelays, and regulation of their activities by phosphatases. In *Bacillus subtilis* and its closest relatives, A.L. Sonenshein, J.A. Hoch, and R. Losick, eds. (Washington: ASM Press), pp. 473–482.
- Piggot, P.J., and Hilbert, D.W. (2004). Sporulation of *Bacillus subtilis*. *Curr. Opin. Microbiol.* **7**, 579–586.
- Piggot, P.J., and Losick, R. (2001). Sporulation genes and intercompartmental regulation. In *Bacillus subtilis* and its closest relatives: from genes to cells, A.L. Sonenshein, J.A. Hoch, and R. Losick, eds. (Washington: ASM Press), pp. 483–517.
- Pogliano, J., Sharp, M.D., and Pogliano, K. (2002). Partitioning of chromosomal DNA during establishment of cellular asymmetry in *Bacillus subtilis*. *J. Bacteriol.* **184**, 1743–1749.
- Rowland, S.L., Burkholder, W.F., Cunningham, K.A., Maciejewski, M.W., Grossman, A.D., and King, G.F. (2004). Structure and mechanism of action of Sda, an inhibitor of the histidine kinases that regulate initiation of sporulation in *Bacillus subtilis*. *Mol. Cell* **13**, 689–701.
- Sambrook, J., Fritsch, E.F., and Maniatis, T. (1989). *Molecular Cloning: A Laboratory Manual* (Cold Spring Harbor, NY: Cold Spring Harbor Laboratory Press).
- Shafikhani, S.H., Nunez, E., and Leighton, T. (2004). Hpr (ScoC) and the phosphorelay couple cell cycle and sporulation in *Bacillus subtilis*. *FEMS Microbiol. Lett.* **231**, 99–110.
- Sharrock, R.A., Rubenstein, S., Chan, M., and Leighton, T. (1984). Intergenic suppression of *spo0* phenotypes by the *Bacillus subtilis* mutation *rvtA*. *Mol. Gen. Genet.* **194**, 260–264.

Smith, B.T., Grossman, A.D., and Walker, G.C. (2001). Visualization of mismatch repair in bacterial cells. *Mol. Cell* 8, 1197–1206.

Sonenshein, A.L. (2000). Control of sporulation initiation in *Bacillus subtilis*. *Curr. Opin. Microbiol.* 3, 561–566.

Sterlini, J.M., and Mandelstam, J. (1969). Commitment to sporulation in *Bacillus subtilis* and its relationship to development of actinomycin resistance. *Biochem. J.* 113, 29–37.

Strahl-Bolsinger, S., Hecht, A., Luo, K., and Grunstein, M. (1997). SIR2 and SIR4 interactions differ in core and extended telomeric heterochromatin in yeast. *Genes Dev.* 11, 83–93.

Webb, C.D., Teleman, A., Gordon, S., Straight, A., Belmont, A., Lin, D.C., Grossman, A.D., Wright, A., and Losick, R. (1997). Bipolar local-

ization of the replication origin regions of chromosomes in vegetative and sporulating cells of *B. subtilis*. *Cell* 88, 667–674.

Weinert, T.A., and Hartwell, L.H. (1988). The RAD9 gene controls the cell cycle response to DNA damage in *Saccharomyces cerevisiae*. *Science* 241, 317–322.

York, K., Kenney, T.J., Satola, S., Moran, C.P., Jr., Poth, H., and Youngman, P. (1992). Spo0A controls the sigma A-dependent activation of *Bacillus subtilis* sporulation-specific transcription unit spoIIIE. *J. Bacteriol.* 174, 2648–2658.

Youngman, P., Perkins, J.B., and Losick, R. (1984). Construction of a cloning site near one end of Tn917 into which foreign DNA may be inserted without affecting transposition in *Bacillus subtilis* or expression of the transposon-borne erm gene. *Plasmid* 12, 1–9.